

# Generation and Investigation of Backscatter Mosaics using TerraSAR-X Data

Paola Rizzoli, Benjamin Bräutigam, Steffen Wollstadt, Josef Mittermayer  
German Aerospace Center (DLR) Oberpfaffenhofen, D-82234 Wessling, Germany

## Abstract

Global backscatter data is required for accurate performance estimation and instrument commanding inside the TerraSAR-X and TanDEM-X missions. The goal of this work is the generation of an X-Band backscatter map by assembling images acquired by the TSX satellite. The complete data ground coverage will be achievable with TanDEM-X mission data. An interpolator, that allows the estimation of the on ground backscatter for any required polarization and incidence angle from the available data, has been implemented too. In this paper, the backscatter map generation algorithm will be presented, together with the first obtained results, generated using TSX data. Moreover, the validity of the interpolation models will also be discussed, presenting a statistical analysis of backscatter behaviour from TSX data.

## 1 Introduction

TerraSAR-X (TSX) and the upcoming twin satellite TanDEM-X (TDX) are two new German SAR satellites, developed in a public/private partnership between DLR and EADS Astrium [1]. The primary target of the TanDEM-X mission is the generation of a worldwide, high precision Digital Elevation Model (DEM), according to the HRTI-3 specification [2]. Both satellites will fly in close orbit configuration, enabling the acquisition of highly accurate cross- and along-track interferograms. A precise information about the Earth's surface and topology is required for many scientific applications, such as hydrology, glaciology, forestry and oceanography. A high accuracy in commanding and performance is needed [3], in order to fulfill such high-demanding tasks. Precise X-Band backscatter data is necessary for an optimized operation of the SAR system. For known backscatter characteristics of a requested SAR scene, the commanded receive gain can be adapted to mitigate clipping or signal saturation. For realistic performance prediction of the SAR and DEM products, the backscatter information is a highly valuable input (e.g. for SNR estimation and height error calculation). Moreover, the availability of a new backscatter map, generated using TSX and, later on, also TDX data, leads to many future scientific applications, such as the monitoring of backscatter evolution in time and the study of reflectivity behaviour depending on the atmospheric conditions. Section 2 shows the map generation algorithm and a preliminary validation using a statistical approach. Section 3 presents the interpolator of missing values, while the first results obtained for the generation of a global X-Band backscatter map are finally displayed in section 4.

## 2 Backscatter Map Algorithm

The complete algorithm for the backscatter map generation can be divided into two main steps: the first one consists in a dedicated processing performed separately on each input product, in order to retrieve a matrix of absolutely calibrated radar brightness values  $\beta^0$ , while the second one is the real assembling of all available data inside the required ground region, generating in such a way the desired output backscatter map.

### 2.1 Step 1: $\beta^0$ Database Generation

Since the total high amount of data to deal with requires the optimization of the processing time and, moreover, high resolution is not needed, TSX quicklook images have been considered as input data [4]. Such images provide less resolution regarding the standard SAR image, by a factor that depends on the acquisition mode. This leads to a pixel spacing of 50 m for ScanSAR (SC), 25 m for Stripmap (SM), 10 m for Spotlight (SL) and 5 m for high resolution Spotlight (HS). The default resolution for the output global backscatter map has been chosen to 5x5 km<sup>2</sup> at the equator. For such a reason, the input quicklook images are first averaged by a factor depending on the acquisition mode, in order to reduce the total amount of data that has to be stored to images of similar resolution. Each sub-sampled image is then geocoded and, for every pixel, the correspondent incidence angle is evaluated. Due to computability costs, an approximation has been done, so that the incidence angles matrix has been estimated taking into account only the sensor position, the desired ground point coordinates and the WGS84 ellipsoid curvature. Moreover, the local slope estimation is not requested, since a mean incidence angle has to be estimated, considering the ground resolution of the averaged input products. Each image is absolutely cal-

ibrated, in order to convert a single pixel digital number  $DN$  into the correspondent radar brightness  $\beta^0$  in the following way:

$$\beta^0 = DN^2/K \quad (1)$$

where  $K$  represents the calibration parameter, obtained from the combination of the processing gain and the TSX calibration constant. It is possible to retrieve the backscatter coefficient  $\sigma^0$  directly from  $\beta^0$ , by compensating the dependence from the local incidence angle  $\alpha$ :

$$\sigma^0 = \beta^0 \sin(\alpha) \quad (2)$$

At this point, every single processed product is stored inside a long term data base, together with some additional parameters connected to it, such as the incidence angles matrix, the geocoded coordinates matrix, the acquisition times and the polarization channel. All these additional parameters are available later on to generate on-demand backscatter maps, for example, using data acquired only inside a certain temporal interval or seasonal period.

## 2.2 Step 2: Mosaic Generation

The generation of the final backscatter map requires the combination of the individual  $\beta^0$  images, generated from the processing chain described in section 2.1. It is well known that, for a given pixel, the amplitude of the radar backscatter depends on several parameters, such as the incidence angle, the surface type, the polarization and the radar frequency. All this factors must be taken into account during the generation process.

The mosaic algorithm flow-chart is described in Figure 1. Once the desired region of interest and other input parameters, such as polarization, reference incidence angle (explained below) and acquisition interval, have been properly set by the user, the  $\beta^0$  database is accessed, to retrieve a list of all the available calibrated data for the required polarization and output map. Since the backscatter amplitude changes depending on the ground characteristics (e.g. type of vegetation, ice-covered regions) and on the incidence angle, it has been decided to refer the output backscatter map to a precise reference incidence angle  $\alpha_{ref}$ , instead of simply applying the angular compensation described in equation 2. For this reason, a dedicated interpolator has been implemented, able to convert  $\beta^0$  values, acquired with different incidence angles, to the reference  $\alpha_{ref}$ . The first step consists in associating to each pixel a proper vegetation class. An AVHRR classification map provided by the USGS, with on-ground resolution of  $1 \times 1 \text{ km}^2$ , has been used [5]. The X-Band backscatter models retrieved from [6] have been used to implement the interpolator. As an example figure 2(a) shows the averaged pixel intensity versus the incidence angle for different vegetation classes and HH polarization. The following function has been used to interpolate the backscatter models:

$$\sigma_0 = c_0 + c_1 \exp(-c_2 \alpha) + c_3 \cos(c_4 \alpha + c_5) \quad (3)$$

where  $c_0, \dots, c_5$ , represent the  $\sigma^0$  fitting coefficients and  $\alpha$  is the incidence angle.

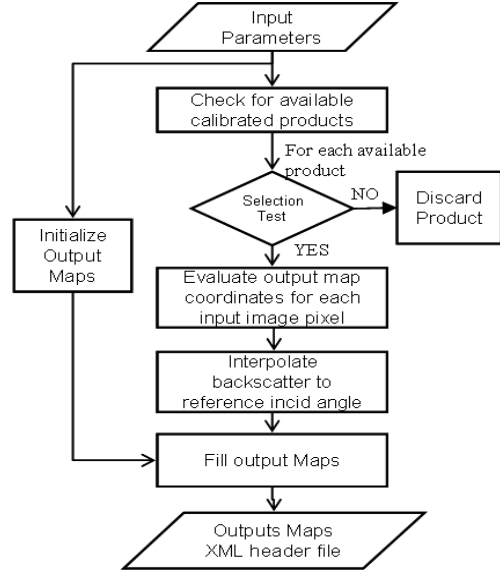


Figure 1: Mosaic Generation flowchart

For each considered vegetation class, a correction curve has been computed, by inverting such models. Applying the proper correction value to each image pixel, depending on the acquisition incidence angle, we are now able to generate a mosaic of  $\sigma^0$  values which is completely referred to a single incidence angle value  $\alpha_{ref}$  (Figure 2(b)).

Notice that more than one pixel can belong to the same output cell. For this reason a proper way to average multiple pixels inside the same cell has been found and three different maps are generated as outputs:

- Backscatter mean value, obtained by averaging all the available calibrated and interpolated values  $\sigma_k^0$  inside a single output resolution cell as:

$$\sigma_{mean}(i, j) = \left( \sum_{k=1}^n \sigma_k^0(i, j) \right) / n \quad (4)$$

where  $i$  represents the row index,  $j$  the column one and  $n$  the total number of input values inside the cell.

- Backscatter maximum value, evaluated as the maximum value of all the available data inside the same output cell:

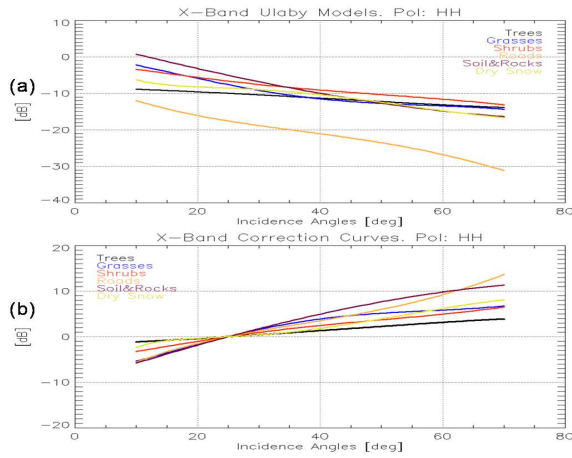
$$\sigma_{max}(i, j) = \max\{\sigma_k^0(i, j)\} \quad k = [1, \dots, n] \quad (5)$$

- Backscatter sample standard deviation, evaluated as:

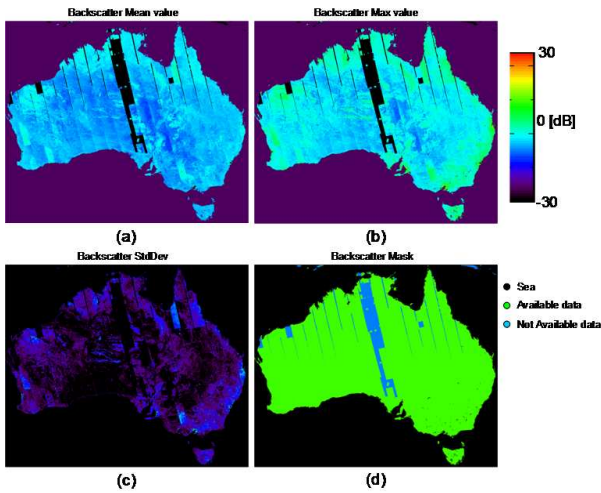
$$\sigma_{sd}(i, j) = \sqrt{\frac{1}{n-1} \left( \sum_{k=1}^n (\sigma_k^0(i, j))^2 - nE[\sigma^0(i, j)]^2 \right)} \quad (6)$$

Figure 3 shows an example of a backscatter map over Australia for a reference incidence angle of 25 [deg] and a sampling step of 0.05 [deg] in lat/lon coordinates. Notice that not all the required data have been acquired yet, so that

some missing values are present, as it can be seen from the data availability mask in figure 3(d).



**Figure 2:** (a) X-Band backscatter dependency with the incidence angle. Ulaby Models (mean value). (b) Correction curves referred to  $\alpha_{ref} = 25$  [deg].



**Figure 3:** Backscattermap example over Australia, HH pol, 25 [deg] incidence. (a) mean value. (b) max value. (c) Standard deviation. (d) Data availability mask.

### 2.3 Backscatter Interpolator Validation

The backscatter map interpolator was implemented taking into account the reflectivity models proposed by F. T. Ulaby in [6]. In order to provide a validation of such models and of the interpolation process itself, a statistical analysis of backscatter reflectivity for TSX data is being performed. Backscatter values coming from different products are analyzed, grouping them together depending on the polarization channel and the vegetation class. In such a way, for a limited number of incidence angles, the histogram of backscatter can be evaluated and compared

with the correspondent Ulaby model, analyzing the accuracy of the interpolation. Figure 4 shows preliminary results obtained considering TSX data acquired with HH polarization and belonging to the vegetation class of *Wooded Grassland*. In this case, backscatter values have been divided into 8 different intervals, depending on the incidence angle, each of them corresponding to a spread of about 5 [deg]. After that, the normalized histograms of backscatter have been evaluated for each interval and fitted using a gaussian distribution. Figure 4(a) presents the results obtained for the intervals of [16.5,21.3] [deg] (black) and of [43.3,48.8] [deg] (red). Notice that the mean backscatter decreases with the increasing of the incidence angle, in fact the gaussian fitting parameters are  $\mu = -9.64$  [dB] (mean value) and  $\sigma^2 = 1.83$  [dB] (variance) for the first set of data and  $\mu = -11.1$  [dB] and  $\sigma^2 = 1.92$  [dB] for the second one. Figure 4(b) shows the mean value (black) and variance (red) of the gaussian fitting for all the 8 considered intervals, together with the corresponding Ulaby model (blue). As it can be seen, a quite good correspondance can be found in this case between the measures and the model.

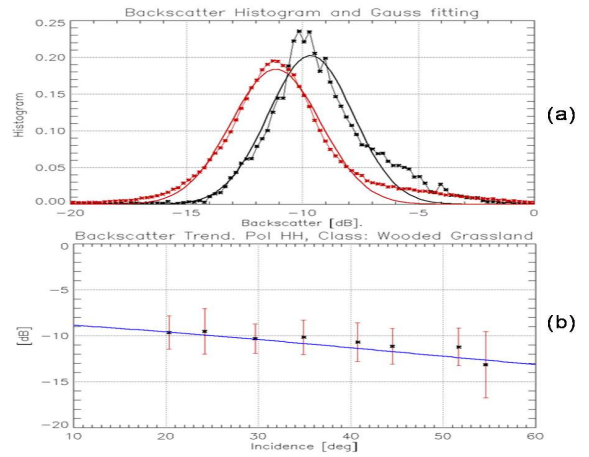


**Figure 4:** X-Band backscatter statistical analysis for *Wooded Grassland* vegetation class and HH polarization. (a) normalized clutter histograms and gaussian fitting. (b) Comparison between gaussian fittings (8 measures) and Ulaby model.

## 3 Interpolation of Missing Values

As noticed in section 2.2, the global earth coverage of TSX data is not available yet. In order to provide a complete map, required i.e. for commanding applications, such areas must be filled. The idea is to use TSX data acquired using different polarizations first and interpolate them for the right polarization and incidence angle in the same way as explained in section 2.2. Then, small gaps can be filled by averaging the nearest available samples. Finally, if empty areas are still present, they can be filled by a coarse C-Band

backscattermap, referred to X-Band. Figure 5(a) shows the backscatter map mean value over Australia after the application of such a processing for an incidence angle of 25 [deg], while figure 5(b) presents a classification mask associated to the interpolated map, that discriminates any different pixel depending on how it was generated.

## 4 Preliminary Results of Global X-Band Backscatter Map

In the current section the preliminary results obtained for the generation of a global X-Band backscatter map are presented. Figure 6 shows the backscatter mean value, generated using all the available TSX data, acquired from October 2008, for HH polarization and a pixel spacing of 0.05 [deg] in lat/lon coordinates (which corresponds to an on-ground resolution of about  $5 \times 5 \text{ km}^2$  at the equator). As it can be seen, many regions, particularly over north America and Asia, have not been acquired yet. Finally, Figure 7 presents the global backscatter map after the application of the interpolation processing for missing values.

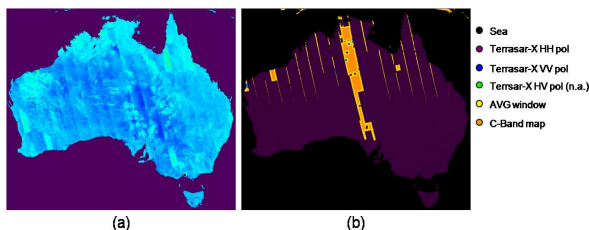


**Figure 5:** Backscattermap example over Australia after *missing values* interpolation, HH pol, 25 [deg] incidence. (a) mean value. (b) Classification mask.

## 5 Conclusion

In this paper, the actual work developed for the generation of X-Band backscatter maps using TSX data has been discussed. The processing approach and the first results obtained for the generation of a global backscatter map, with on ground resolution of  $5 \times 5 \text{ km}^2$  at the equator, have been presented. Nevertheless, on demand backscatter maps, characterized by higher resolution, can be generated as well. Not enough data have been acquired with TSX yet, to generate a complete global backscatter map, covering the whole earth. The full coverage will be achieved with the systematic acquisitions provided during the TanDEM-X mission. The importance of having a complete global backscatter map resides in the many further applications that require its use, such as instrument commanding and performance estimation. For this reason an interpolator has been implemented, filling gaps with corrected data from other polarizations, neighbor samples or even other sensors. The validation of the entire process is under testing and a statistical analysis of the X-Band backscatter behaviour is being performed.

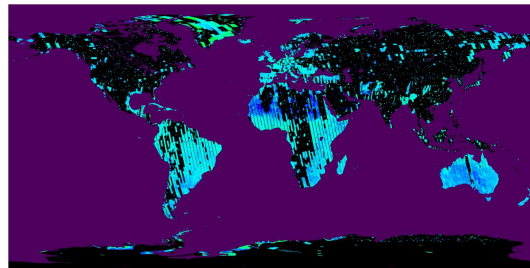


**Figure 6:** X-Band global backscattermap (mean value) for HH polarization, generated using all the TSX available quicklook data, acquired from October 2008. Values are saturated inside the interval of  $[-30, +30]$  dB.

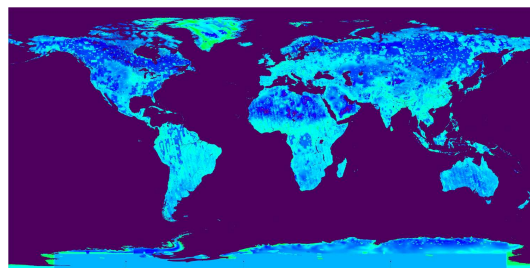


**Figure 7:** X-Band global backscattermap (mean value) for HH polarization, after the application of the missing values interpolator of missing values.

## References

- [1] Buckreuss S.; Werninghaus R.; Pitz W.: *German Satellite Mission TerraSAR-X*, 2008 IEEE Conference, Rome, Italy, 2008
- [2] Krieger G.; Moreira A.; Fiedler H.; Hajnsek I.; Werner M.; Younis M.; Zink M.: *TanDEM-X: A Satellite Formation for High-Resolution SAR Interferometry*, IEEE Transactions on Geos. and Remote Sens., vol. 45, no. 11, pp. 3317-3341, Nov. 2007
- [3] Mittermayer J.; Younis M.; Metzger R.; Wollstadt S.; Márquez J.; Meta A.: *TerraSAR-X System Performance Characterization and Verification*, IEEE Trans. Geosci. Remote Sens., vol. 48, no. 2, Feb. 2010. To be published.
- [4] Fritz T.; Eineder M.; Breit H.; Schättler B.; Boerner E.; Huber M.: *The TerraSAR-X Basic Products - Format and Expected Performance*, Eusar Proceedings, 2006
- [5] <http://edc2.usgs.gov/1km/1kmhomepage.php>
- [6] Ulaby F. T.; Dobson M. C.: *Handbook of Radar Scattering Statistics for Terrain*, Norwood, MA: Artech House, 1989